JOURNAL OF THERMOPHYSICS AND HEAT TRANSFER
Vol. 12, No. 2, April–June 1998

Experimental and Numerical Study of Nonequilibrium Ultraviolet NO and N_2^+ Emission in Shock Layer

V. A. Gorelov,* M. K. Gladyshev,† A. Y. Kireev,† and I. V. Yegorov†
Central Aerohydrodynamic Institute, Zhukovsky-3, Moscow Region 140160, Russia
and
Y. A. Plastinin‡ and G. F. Karabadzhak§
Central Research Institute of Machine Building, Korolev, Moscow Region 141070, Russia

The results on an investigation of nonequilibrium uv radiation in the systems of molecular bands NO and $N_2^+(1-)$ in a shock layer in air are presented. The studies included the experiments on a measurement of the nonequilibrium radiation behind a strong shock wave in an electric arc-driven shock tube within the range of shock-wave velocity change V_s = 5 to 10 km/s at the initial air pressure P_1 = 0.1 torr, and numerical simulation of radiation processes behind the shock wave and in a hypersonic viscous shock layer, where the flow was simulated on the basis of Navier–Stokes equations. A numerical model of the radiation behind the strong shock wave has been used to verify a kinetic scheme of radiation processes by comparison with experimental results. Examples of emission calculations in the NO and $N_2^+(1-)$ systems for the conditions of a flight test are presented.

Nomenclature

B	=	rotational constant
c	=	speed of light, cm/s
D	=	energy of dissociation, K
e	=	electron
H	=	flight altitude, km
h	=	Planck's constant
I	=	radiation intensity, W/cm^3 sr μm
k	=	rate constant of reaction
m	=	mass, g
n	=	concentration, cm^{-3}
P	=	pressure, torr
R	=	radiance, W/cm^2 sr μm
T	=	temperature, K
t	=	time, s or μs
U	=	rate of electron energy exchange
V	=	flight or shock wave velocity, km/s
v	=	vibrational number
x	=	distance behind shock wave, cm
y	=	stagnation line distance, cm
β, γ	=	parameters in vibration–dissociation model
λ	=	wavelength, nm or μm
θ	=	characteristic vibrational temperature, K
ν	=	collision frequency, s^{-1}
σ	=	cross section, cm^2
τ	=	time, lifetime, s, ns, or μs
ω_0, $\omega_0 x_0$, $\omega_0 y_0$, $\omega_0 z_0$	=	vibrational constants

Subscripts

ai	=	associative ionization
e	=	electron, electronic
el	=	elastic
f	=	forward
m	=	maximum
R	=	rotational
r	=	reverse
s	=	shock-wave condition
v	=	vibrational
1	=	condition ahead of a shock wave
∞	=	freestream condition

Superscripts

′	=	upper excited state
″	=	lower excited state

Presented as Paper 96-1900 at the AIAA 31st Thermophysics Conference, New Orleans, LA, June 17–20, 1996; received July 2, 1996; revision received July 15, 1997; accepted for publication Aug. 7, 1997.

*Deputy Head, Hypersonic Department, and Head, Aerophysical Division. Member AIAA.
†Leading Scientist, Aerophysical Division.
‡Head of Division, Heat Transfer Department. Member AIAA.
§Head of Laboratory, Heat Transfer Department. Member AIAA.

Introduction

RECENTLY, there has been a wave of interest in nonequilibrium hypersonic viscous shock layer radiation studies. The main direction of these studies is to specify numerical models of nonequilibrium processes in a shock layer within a wide range of flight altitudes and speeds. An important stage is the experimental verification of the used kinetic models. Flight tests performed on bow shock flight experiments[2] made it possible to revise a model of radiation processes in a shock layer at flight velocities V = 3.5 and 5.1 km/s. The flight experiment makes it possible to obtain very valuable information on a study of nonequilibrium processes in a viscous shock layer within a wide range of flight altitudes. The possibilities to verify numerical models can be expanded when the results on radiation measurements in laboratory experiments are also used. In this way, the numerical model of the flow behind the shock wave is compared with the data measured in a shock tube. A model verified like this can be used for numerical simulation of the radiation in a viscous shock layer. Then a comparison with flight data can be performed. Such an approach has been used in this work to get results, some of which are presented in the following text. A numerical model of radiation in the NO and $N_2^+(1-)$ systems in a viscous shock layer has been developed. Some parts of this model differ from the models used in Refs. 1 and 2. A kinetic scheme of radiation processes has been verified by using the results of a number

of experiments performed in the electric arc-driven shock tube (EAST).[3]

Main attention was paid to the study of shock-layer radiation when shock velocity was about 8 km/s, but a number of calculations were performed for flight conditions when V = 3.5 and 5.1 km/s. The experiments were performed within the changing range of shock-wave velocities V_s from 5 to 10 km/s.

Experiment Description

Experimental investigations of the radiation behind a strong shock wave have been performed in the EAST, where a series of investigations of the processes behind strong shock waves in the air were carried out.[4] The discharge driver chamber of the EAST had ceramic walls and molibden electrodes. Driver gas was helium heated by an electric discharge. A low-pressure-driven channel was assembled from glass sections (the length was ~5 m and the diameter was 57 mm). It was preliminarily evacuated up to a pressure of 10^{-3} torr. Dry air was delivered through the capillary into the channel at its end. A continuous air evacuation was performed at a specified value of P_1 in the channel. Thus, the level of impurities in the gas under study has been reduced. The velocity of shock-wave propagation was measured by a system of photomultipliers with an accuracy of about 1%. The routine test scheme to measure the radiation intensity behind the shock wave was described in Ref. 5. A diffraction monochromator with the photomultipliers was used to measure the emission in spectral intervals. The temporal resolution of the measured system was about 0.1 μs. Measurements of I were performed within the following spectral intervals and values of P_1 and V_s.

- λ about 235.0 nm—system NO, P_1 = 0.1 torr, V_s = 5–10 km/s
- λ about 391.4 nm—system $N_2^+(1-)$, P_1 = 0.1, torr, V_s = 7–11 km/s

For λ = 391.4 nm, the measurements performed in the EAST for V_s = 10.1 km/s and P_1 = 0.1 torr were in a good agreement with the data obtained in Ref. 6. The level of radiation in the spectral range λ = 385 ± 2.5 nm (CN molecular band system) in our experiments was lower than measured in Ref. 6.

Kinetical Model

The targets of numerical modeling are the verification of calculations by experimental results and the correction of a used kinetical model. Numerical simulation of nonequilibrium air radiation is based upon using a physical–chemical model of high-temperature air and the models of nonequilibrium radiation formation. The air under conditions of high-temperature shock layer at considered velocities and altitudes is a mixture of species: N_2, O_2, NO, N, O, NO^+, N_2^+, O_2^+, O^+, N^+ and electrons e. To simulate the nonequilibrium radiation formation in the band systems of molecules and molecular ions, the previously considered gas mixture is supplemented by corresponding species in excited electronic–vibrational–rotational states. The multitemperature model for vibrational relaxation when vibrational temperatures of molecules differ from one another is used in kinetical model. It is assumed that rotational degrees of freedom molecules in the ground state are in equilibrium with a translational degrees of freedom gas mixture.

Vibrational Relaxation

To describe the vibrational excitation of N_2 and O_2 molecules, the model from Ref. 7 is used. The relaxation time τ may be calculated from correlation $p\tau = AT^n \exp(BT^{-1/3})$, where values of A (in μs atm), n, and B coefficients are presented in Table 1.

Vibrational excitation of the NO molecule was calculated by using the relaxation time from Ref. 8. The excitation of N_2 vibrational levels by electron impact is given by the following reaction[9]:

$$N_2(v) + e \rightleftarrows N_2^- \rightleftarrows N_2(v') + e \tag{1}$$

The influence of reaction (1) on the vibrational relaxation of the N_2 molecule was taken into account by the model,[10] using rate constants of a step-by-step population of N_2 vibrational levels.[9] Reaction (1) carries an important contribution into the energy balance of electron gas and determines in a great part the distribution of electron temperature in a shock layer (see the Electron Temperature section).

Table 1 Relaxation time coefficients

Process	M	A	n	B
$O_2(v = 1) + M$	N_2	4.66×10^{-36}	5.99	511.1
	O_2	1.1×10^{-25}	4.235	354.0
	NO	3.2×10^{-41}	6.875	592.6
	N	1.4×10^{-37}	6.298	528.7
	O	8.9×10^{-29}	4.862	353.2
$N_2(v = 1) + M$	N_2	3.3×10^{-29}	4.555	523.9
	O_2	7.6×10^{-44}	7.104	717.8
	NO	1.0×10^{-43}	7.088	712.9
	N	5.0×10^{-40}	6.446	848.6
	O	7.6×10^{-41}	6.291	662.3

Dissociation of Diatomic Molecules

The dissociation of N_2, O_2, and NO molecules proceeds simultaneously with their vibrational excitation in considered temperature diapason. This fact stipulates the close interaction and a interinfluence between a vibrational relaxation of molecules, their dissociation, and a recombination of atoms into a molecule. An influence of nonequilibrium excitation of vibration degrees of freedom on the rates of dissociation reactions were taken into account by a two-temperature dependence of the rate constant[7] $k(T, T_v) = k_0(T) \cdot \Phi(T, T_v)$. The function $\Phi(T, T_v)$ was determined on the model base of an effective vibration level that is distant from the dissociation limit on the value of βT (the β model of dissociation), by the following formula:

$$\Phi(T, T_v) = \frac{1 - \exp(-\theta/T_v)}{1 - \exp(-\theta/T)} \exp\left[-(D - \beta T)\left(\frac{1}{T_v} - \frac{1}{T}\right)\right]$$

The values of D and β for O_2, 59,400 K and 1.5; for N_2, 113,200 K and 3.0; and for NO, 75,500 K and 3.0.[7] The dissociation reactions taken into account are shown in Table 2.

NO Formation

NO molecules are more efficiently formed through exchange chemical reactions:

$$N_2(v) + O \rightleftarrows NO + N \tag{2}$$

$$O_2 + N \rightleftarrows NO + O \tag{3}$$

Note that the exchange chemical reactions have an important meaning in numerical simulations of a radiation in molecular bands of NO, because the total product of NO depends upon the accuracy of these reactions' description. According to Ref. 7, reaction (2) may proceed with the participation of a vibrationally excited N_2 molecule. In this case, the rate constant of Eq. (2) depends upon vibrational temperature $T_{v_{N_2}}$ and upon translational temperature T as follows:

$$k(T, T_{v_{N_2}}) = \frac{6.8 \times 10^{13}}{Q(T_{v_{N_2}})} \sum_v \exp\left[\left(\frac{E_a}{T} - \frac{E_v}{T_{v_{N_2}}}\right) - \frac{(E_a - \gamma E_v)}{\beta T} \cdot \Theta \cdot (E_a - \gamma E_v)\right]$$

Table 2 Reactions of dissociation

Reaction	M	k_0, cm^3/mol·s	Reference
$N_2(v) + M \rightleftarrows N + N + M$	N_2	$4.9 \times 10^{17} \cdot T^{-0.5} \cdot \exp(-113{,}200/T)$	11
	N	$7.4 \times 10^{18} \cdot T^{-0.5} \cdot \exp(-113{,}200/T)$	11
	O, O_2, NO	$1.8 \times 10^{17} \cdot T^{-0.5} \cdot \exp(-113{,}200/T)$	11
	e	$8.1 \times 10^{19} \cdot T_e^{-1.28} \cdot \exp(-113{,}200/T_e)$	7
$O_2(v) + M \rightleftarrows O + O + M$	O_2	$3.25 \times 10^{19} \cdot T^{-1} \cdot \exp(-59{,}380/T)$	11
	O	$8.10 \times 10^{19} \cdot T^{-1} \cdot \exp(-59{,}380/T)$	11
	N, N_2, NO	$6.15 \times 10^{18} \cdot T^{-1} \cdot \exp(-59{,}380/T)$	11
	e	$1.0 \times 10^{-25} \cdot T_e^{7.9} \cdot \exp(-70{,}760/T_e)$	7
$NO(v) + M \rightleftarrows N + O + M$	N_2, O_2, N, O, NO	$4 \times 10^{20} \cdot T^{-1.5} \cdot \exp(-75{,}400/T)$	11
	e	$4.68 \times 10^{9} \cdot T_e^{1.34} \cdot \exp(-78{,}530/T_e)$	7

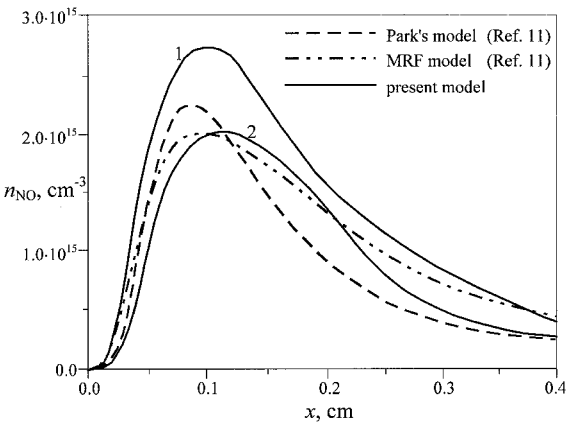

Fig. 1 NO-formation behind shock wave (V_s 5 9 km/s, P_1 5 0.04 torr). Rate constant of reaction (2): from Ref. 12, curve 1; from Ref. 7, curve 2.

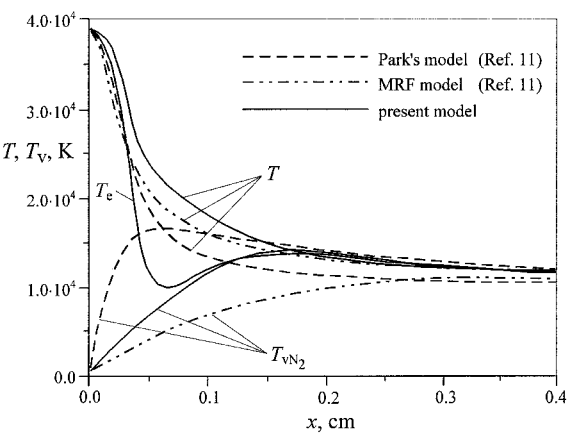

Fig. 2 Temperatures distributions behind shock wave (V_s 5 9 km/s, P_1 5 0.04 torr).

where E_a = 38,000 K; β = 0.9; γ = 0.52; $Q(T_{vN_2}) = [1 - \exp(-D/T_{vN_2})]/[1 - \exp(-\theta/T_{vN_2})]$. Θ is the Heaviside function, E_v is the vibrational energy of the N_2 molecule, corresponding to v, and D is the dissociation energy of nitrogen. The rate constant of reaction (3) has a $k_f = 6.4 \times 10^9 \, T \cdot \exp(-3150/T)$ cm^3/mol·s form.[7]

Figure 1 shows the comparison of nitric oxide density calculations using different rate constants of reaction (2) and the results presented in Ref. 11. Note that the prediction of NO formation by the Macheret–Fridman–Rich (MFR) model and our results are very close (Fig. 1). The use of the rate constant of reaction (2), recommended in Ref. 12, in this computational model results in an increase of NO peak concentration. The distributions of translational T and nitrogen vibrational T_{vN_2} temperatures calculated with the use of the described kinetical model, and results from Ref. 11 are shown in Fig. 2. A difference is noted between the nitrogen vibrational temperature distributions calculated in Ref. 11 using different models. Our calculated data lie between Park's model and the MRF model results presented in Ref. 11. Note, that the difference in vibrational temperature distributions don't considerably effect the NO concentration.

Ionization

It is assumed that electrons in a shock layer are formed at flow velocities through three associative reactions of ionization and reactions of ionization by an electron impact (Table 3).

The rate constants are the functions of electron temperature, which differs from translational and vibrational temperatures.

Electron Temperature

Electron temperature T_e is defined from a balance equation of electron energy:

$$\frac{\mathrm{d}}{\mathrm{d}t}\left(\frac{3}{2} T_e n_e\right) = U_{ai} - U_{el} - U_{e-R} - U_{e-v}$$

The following electron energy exchange processes were taken into account in a balance equation of electron energy:

1) The appearance of electrons with the energy $E \sim kT$ through associative ionization reactions[13] and the loss of electron energy in the recombination reactions of ions and electron

$$U_{ai} = \frac{3}{2} \sum_{j=1}^{3} (T \cdot R_{fj} - T_e \cdot R_{rj})$$

where R_{fj} and R_{rj} are the forward and reverse rates of associative ionization reaction j, respectively.

2) The energy exchange in elastic collisions between the electron and heavy particle i

$$U_{el} = \sum_i \frac{3m_e}{m_i} \nu_{ei} n_e (T - T_e)$$

where ν_{ei} is the collision frequency, and m_e and m_i are the electron and heavy particle i masses, respectively.

3) Electron energy exchange with rotational degrees of freedom molecules.[14]

$$U_{e-R} = \sum_{j=1}^{3} \frac{64}{\sqrt{3}} B_j \left(\frac{8kT_e}{\pi m_e}\right)^{0.5} \sigma_R \left(\frac{T}{T_e} - 1\right) \cdot n_j n_e$$

where k is the Boltzmann's constant, $\sigma_R = 2\pi s_j^2/15ea_0^2$ is the cross section, s_j is the molecular quadrupole moment, and B_j is the rotational constant of the molecular species j (N_2, O_2, and NO).

Table 3 Reactions of ionization

Reaction	k_{fr}, cm^3/mol·s	Reference
$N + O \rightleftarrows NO^+ + e$	$k_r = 2.6 \times 10^{19} \cdot T_e^{-1}$	7
$N + N \rightleftarrows N_2^+ + e$	$k_r = 5.0 \times 10^{18} \cdot T_e^{-1/2}$	7
$O + O \rightleftarrows O_2^+ + e$	$k_r = 5.0 \times 10^{19} \cdot T_e^{-1}$	7
$NO + \rightleftarrows e \rightleftarrows NO^+ + e + e$	$k_f = 6.5 \times 10^{23} \cdot T_e^{-1.7} \cdot \exp(-107{,}370/T_e)$	7
$N_2 + e \rightleftarrows N_2^+ + e + e$	$k_f = 4.5 \times 10^{-7} \cdot T_e^{5} \cdot \exp(-118{,}840/T_e)$	7
$O + e \rightleftarrows O^+ + e + e$	$k_f = 5.2 \times 10^{12} \cdot T_e^{0.67} \cdot \exp(-157{,}980/T_e)$	7
$O_2 + e \rightleftarrows O_2^+ + e + e$	$k_f = 1 \times 10^{-13} \cdot T_e^{6} \cdot \exp(-140{,}150/T_e)$	7
$N + e \rightleftarrows N^+ + e + e$	$k_f = 1.8 \times 10^{13} \cdot T_e^{0.6} \cdot \exp(-168{,}770/T_e)$	7

Table 4 Rate constant coefficients for reaction (1)[a]

v	0	0	1	0	1	2	0	1	2	3
v'	1	2	2	3	3	3	4	4	4	4
A	83	63	116	58	169	35	49	147	24	54
n	−0.5	−1.1	−1.3	−1.5	−1.4	−1.0	−1.5	−1.5	−1.0	−1.2
C	1.7	1.9	2.0	2.3	2.0	1.5	2.4	2.1	1.4	1.3

[a] $k_{vv'}(T_e) = AT_e^n \exp(-C/T_e)$, where A is in 10^{-10} cm^3/s and T_e and C are in eV.

Table 5 Charge-exchange reactions

Reaction	k_f, cm^3/mole·s	Reference
$O_2^+ + N_2 \rightleftarrows O_2 + N_2^+$	$9.9 \times 10^{12} \cdot \exp(-40{,}700/T)$	7
$NO^+ + N_2 \rightleftarrows NO + N_2^+$	$3.8 \times 10^{15} \cdot \exp(-73{,}230/T)$	7
$O_2^+ + N \rightleftarrows O_2 + N^+$	$8.7 \times 10^{13} \cdot T^{0.14} \cdot \exp(-28{,}600/T)$	7
$O_2 + O^+ \rightleftarrows O_2^+ + O$	$6.45 \cdot 10^{14} \cdot T^{0.7}$	7
$O^+ + N_2 \rightleftarrows O + N_2^+$	$9.0 \times 10^{11} \cdot T^{0.36} \cdot \exp(-22{,}800/T)$	7
$NO^+ + O \rightleftarrows NO + O^+$	$1.82 \times 10^{13} \cdot \exp(-50{,}130/T)$	7
$NO^+ + O_2 \rightleftarrows NO + O_2^+$	$2.4 \times 10^{13} \cdot \exp(-32{,}600/T)$	7
$N_2^+ + O \rightleftarrows NO + N^+$	$1.8 \times 10^{14} \cdot \exp(-25{,}760/T)$	7
$N_2 + O^+ \rightleftarrows NO + N$	$2.2 \times 10^{14}/T$	8
$NO^+ + N \rightleftarrows O + N_2^+$	$7.2 \times 10^{13} \cdot \exp(-35{,}500/T)$	7
$NO^+ + O \rightleftarrows O_2 + N^+$	$10^{12} \cdot \sqrt{T} \cdot \exp(-77{,}200/T)$	7
$NO + O^+ \rightleftarrows O_2 + N^+$	$1.4 \times 10^{5} \cdot T^{1.9} \cdot \exp(-15{,}300/T)$	7

4) Excitation of vibrational levels of the N_2 molecule through reaction (1)

$$U_{e-V} = \frac{n_e n_{N_2}}{q} \sum_{v=0}^{8} v\theta_{N_2} \left\{ \exp\left(-\frac{v\theta_{N_2}}{T_e}\right) \times \sum_{v'=1}^{9} k_{vv'}(T_e) \cdot \exp\left[\frac{v'\theta_{N_2}(T_{vN_2} - T_e)}{T_{vN_2} T_e}\right] - \exp\left(-\frac{v\theta_{N_2}}{T_{vN_2}}\right) \cdot \sum_{v'=1}^{9} k_{vv'}(T_e) \right\}$$

where q is the vibrational N_2 partition function, and $k_{vv'}(T_e)$ is the rate constants for reaction (1) ($v < v'$).

The Arrhenius form approximation[10] on the rate constant calculations are presented in Table 4 for v and v' and an electron energy diapason from 0.5 to 3.0 eV.

Process (1) determines, in general, the T_e distribution under conditions of a weak dissociation of N_2. The calculated T_e distribution behind the steady-state shock wave is presented in Fig. 2. The peak value of the electron temperature approximately equals the translational temperature. The presence of T_e − peak value in the shock front was also determined in Refs. 4 and 15. Because of the influence of the electron–vibration energy exchange in reaction (1) on the electron energy, T_e relaxes to a nitrogen vibrational temperature in a relatively thin zone behind the shock front.

Charge Exchange Reaction

Positive charged species (atoms and molecules) exchange by charge with neutral plasma components through the reactions presented in Table 5.

Model of Radiation

Radiation Intensity

To calculate a radiation intensity I of molecular bands, the following simplified formula is used[16]:

$$I = 4.6 \times 10^{-4} \frac{1}{\Delta\lambda g'_e} \int_{\lambda - \Delta\lambda/2}^{\lambda + \Delta\lambda/2} \frac{d\lambda'}{\lambda'^6} \sum_{v',v''} n_{v'} \frac{S_{e,v'v''} q_{v'v''} B_{v'}}{T_R |B_{v'} - B_{v''}|} \times \exp\left[-\frac{hc}{k} \cdot \frac{B_{v'} \times 10^4}{T_R} \cdot \left(\frac{1}{\lambda'} - \frac{1}{\lambda_{v'v''}}\right) \cdot \frac{1}{B_{v'} - B_{v''}}\right] \quad (4)$$

The sum is made for all vibrational numbers v', v'' if $(B_{v'} - B_{v''}) \times (1/\lambda - 1/\lambda_{v'v''}) > 0$, where v', v'' are vibrational quantum numbers of upper and lower electronic states, and $\lambda_{v'v''}$ is a wavelength of transition band center (v', v''):

$$\lambda_{v'v''} = \frac{10^4}{10^4/\lambda_{00} + G_0(v') - G_0(v'')}.$$

$\Delta\lambda$ is the mean interval (it was assumed that $\Delta\lambda = 0.1$ nm), λ_{00} is the center of the electronic band system, $G_0(v) = \omega_0 v - \omega_0 x_0 v^2 + \omega_0 y_0 v^3 + \omega_0 z_0 v^4$ is the vibrational state energy (cm^{-1}), g_e is the degeneracy of electronic state, $B_v = B_e - \alpha_e(v + 1/2)$ (cm^{-1}) where B_e and α_e are rotational constants, and $S_{e,v'v''}$ is the strength of an electronic transition (atomic units). The function $S_{e,v'v''} = S_{e,v'v''}(\lambda)$ is taken into account in calculations[17] and $q_{v'v''}$ Frank-Condon factors.[18] T_R is a rotational temperature (in calculations $T_R = T$), and $n_{v'}$ is a concentration of molecules in an upper electronic–vibrational excited state. The distribution among vibrational levels within an electronic state of molecules is assumed to be Boltzmann's with a vibrational temperature T_v of the ground electronic state of molecules. According to for-

Table 6 Reactions of NO excited states formation

Reaction	k_f, cm^3/mol·s or cm^6/mol^2·s	Reference
$N + O + N_2 \rightleftarrows NO(A) + N_2$	$7.7 \times 10^{13} \cdot (T/300)^{-1.24}$	20
$N + O + N_2 \rightleftarrows NO(B) + N_2$	$1.9 \times 10^{13} \cdot (T/300)^{-1.4}$	20
$N + O \rightleftarrows NO(A)$	$7.1 \times 10^{6} \cdot (T/300)^{-0.35}$	20
$N + O \rightleftarrows NO(C)$	$4.1 \times 10^{6} \cdot (T/300)^{-0.35}$	20
$NO(A) + M \rightleftarrows NO(X) + M$	$5.20 \times 10^{12} \cdot T^{0.5}$	21
$NO(B) + M \rightleftarrows NO(X) + M$	$6.40 \times 10^{12} \cdot T^{0.5}$	21
$NO(C) + M \rightleftarrows NO(X) + M$	$7.56 \times 10^{12} \cdot T^{0.5}$	21
$NO(X) + e \rightleftarrows NO(A) + e$	$7.20 \times 10^{13} \cdot \exp(-63{,}500/T_e)$	22
$NO(X) + e \rightleftarrows NO(B) + e$	$6.10 \times 10^{13} \cdot \exp(-65{,}700/T_e)$	22
$NO(X) + e \rightleftarrows NO(C) + e$	$8.40 \times 10^{13} \cdot \exp(-74{,}300/T_e)$	22
$NO(A) + e \rightleftarrows NO(B) + e$	1.20×10^{15} (estimation)	23
$NO(B) + e \rightleftarrows NO(C) + e$	4.10×10^{15} (estimation)	23
$NO(A) \rightarrow NO(X) + h\nu(\gamma)$	$\tau = 0.2$ μs	17
$NO(B) \rightarrow NO(X) + h\nu(\beta)$	$\tau = 3.0$ μs	17
$NO(C) \rightarrow NO(X) + h\nu(\delta)$	$\tau = 30$ ns	17

Table 7 Reactions of $N_2(A^3\Sigma_u^+)$ formation

Reaction	k_f, cm^3/mol·s or cm^6/mol^2·s	Reference
$N_2(X) + N_2 \rightleftarrows N_2(A) + N_2$	$1.1 \times 10^{12} \cdot T^{-0.5} \cdot \exp(-71{,}600/T)$	26
$N_2(X) + N \rightleftarrows N_2(A) + N$	$1.2 \times 10^{17} \cdot T^{-1.5} \cdot \exp(-71{,}600/T)$	26
$N_2(X) + O \rightleftarrows N_2(A) + O$	$7.2 \times 10^{16} \cdot T^{-1.5} \cdot \exp(-71{,}600/T)$	26 and 27
$N_2(X) + O_2 \rightleftarrows N_2(A) + O_2$	$6.0 \times 10^{15} \cdot T^{-1.5} \cdot \exp(-71{,}600/T)$	26 and 27
$N + N + N_2 \rightleftarrows N_2(A) + N_2$	$0.8 \times 10^{17} \cdot T^{-0.8}$	28
$N + N \rightleftarrows N_2(A)$	$4.9 \times 10^{7} \cdot T^{-0.35}$	27
$N_2(A) + N_2(A) \rightleftarrows N_2(B) + N_2(X, v)$	7.4×10^{14}	29
$N_2(X) + e \rightleftarrows N_2(A) + e$	$6.14 \times 10^{15} \cdot \exp(-71{,}600/T_e)$	30
$N_2(A) + e \rightleftarrows N_2(B) + e$	1.81×10^{14}	31

mula (4), to calculate the radiation intensity in molecular band systems, it is necessary to have the information about the vibrational and translational temperatures and the population of the upper electronic state of transition distributions in a high-temperature shock layer. The densities of excited states of molecules are obtained by solving the master equations written analogous to species master equations.[19]

Nitric Oxide Band System

The numerical simulation of a radiation in the NO band system is made for the following:

Radiation of β band ($B^2\Pi$, $v' \rightarrow X^2\Pi$, v''), 180 nm < λ < 400 nm
Radiation of γ band ($A^2\Sigma^+$, $v' \rightarrow X^2\Pi$, v''), 195 nm < λ < 340 nm
Radiation of δ band ($C^2\Pi$, $v' \rightarrow X^2\Pi$, v''), 184 nm < λ < 210 nm
Radiation of ε band ($D^2\Sigma^+$, $v' \rightarrow X^2\Pi$, v''), 170 nm < λ < 190 nm

Considerable concentrations of NO in a shock layer and small lifetimes of excited states NO(A), NO(C), and NO(D) predict the presence of high radiation intensity values in NO(γ, δ, ε) band systems. The reaction scheme of A, B, and C levels of NO from Table 6 is used to simulate nonequilibrium radiation in the present numerical model.

In Table 6, NO(X) ≡ NO($X^2\Pi$); NO(A) ≡ NO($A^2\Sigma^+$); NO(B) ≡ NO($B^2\Pi$); NO(C) ≡ NO($C^2\Pi$); NO(D) ≡ NO($D^2\Sigma$). In addition to the reactions in Table 6, the following resonance reactions are of great importance in the process of $A^2\Sigma^+$ and $C^2\Pi$ NO levels population:

$$NO(X) + N_2(A) \rightleftarrows NO(A, v) + N_2(X) \qquad (5)$$

$$NO(X) + N_2(A) \rightleftarrows NO(C, v) + N_2(X) \qquad (6)$$

The rate constant of reaction (5) is varied from 6.02×10^{13} cm^3/mol·s to 10^{13} cm^3/mol·s (Ref. 24). The value of k_f = 6.02×10^{13} cm^3/mol·s, (Ref. 25) is used in our model. The rate constant of reaction (6) is from Ref. 21, $k_f = 5.8 \times 10^{14}$ cm^3/mol·s. Reactions (5) and (6) couple the population of $N_2(A)$ electronic state and NO(γ), NO(δ) emission. This fact leads to the necessity of coupling the nonequilibrium population of $N_2(A)$ kinetics and the uv NO γ, δ emission. The kinetical scheme for the $N_2(A)$ electronic level population was added to the previously described NO(A, B, C) formation model. The reactions of $N_2(A^3\Sigma_u^+)$ excitation from Table 7 were taken into account in the calculations.

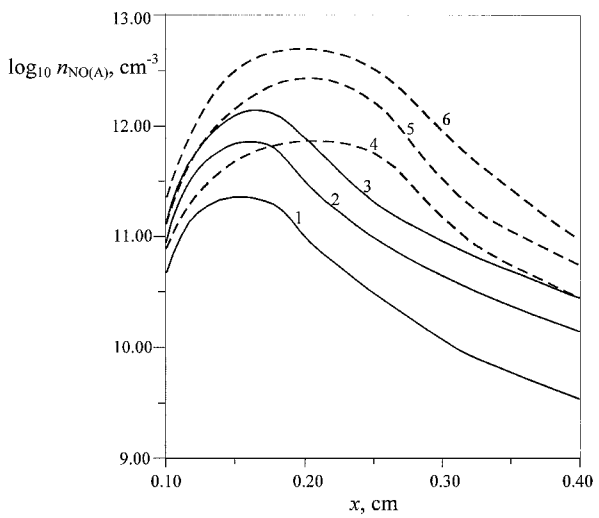

Fig. 3 NO(A) concentration behind a shock wave as a function of rate constants of reactions (2) and (5) variation (V_s 5 8 km/s, P_1 5 0.1 torr).

To evaluate the radiation in NO(ε) band systems, the assumption about Boltzmann's equilibrium distribution-excited NO molecules on $D^2\Sigma$ and $C^2\Pi$ levels is used. Figure 3 shows the influence of the rate constant variation of reactions (2) and (5) on the NO(A) population. The rate constant for curves 1

Table 8 Reactions of $N_2^+(B^2S_u^+)$ formation

Reaction	k_f, cm^3/mol·s	Reference
$N_2(X, v > 12) + N_2^+(X) \rightleftarrows N_2^+(B) + N_2(X, v' = 0)$	$1.5 \times 10^{14} \cdot \exp(-800/T)$	26
$N_2^+(X) + e \rightleftarrows N_2^+(A) + e$	$4.3 \times 10^{13} \cdot \exp(-13{,}300/T_e)$	23
$N_2^+(X) + e \rightleftarrows N_2^+(B) + e$	$5.6 \times 10^{15} \cdot T_e^{-0.5} \cdot \exp(-36{,}800/T_e)$	32
$N_2^+(A) + e \rightleftarrows N_2^+(B) + e$	$6.1 \times 10^{14} \cdot \exp(-23{,}500/T_e)$	23
$N_2^+(B) \rightarrow N_2^+(X) + h\nu$	$\tau = 65$ ns	17

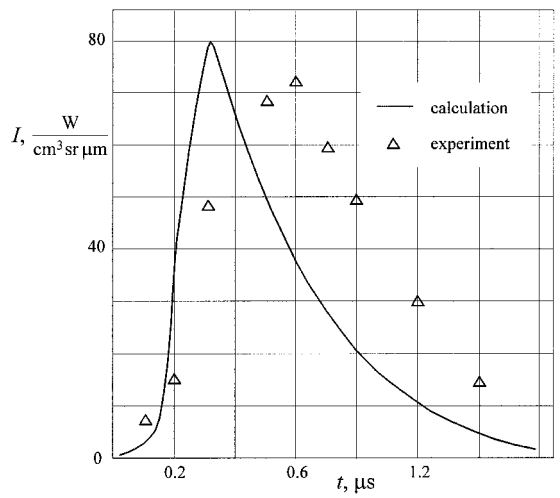

Fig. 4 Experimental and calculated NO(g) radiation behind a shock wave: l = 235 ± 7 nm (V_s = 8 km/s, P_1 = 0.1 torr).

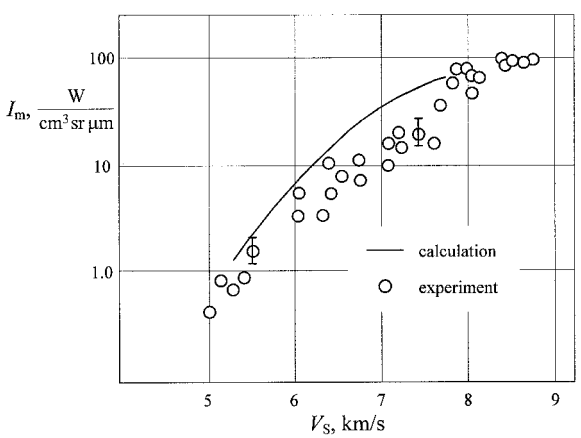

Fig. 5 NO(g) radiation intensity peak as a function of shock-wave velocity: l = 235 ± 7 nm, P_1 = 0.1 torr.

and 4 was $k_f = 10^{13}$ cm^3/mol·s; for curves 2 and 5, $k_f = 6.02 \times 10^{13}$ cm^3/mol·s; and for curves 3 and 6, $k_f = 10^{14}$ cm^3/mol·s. Data shown by curves 4–6 were calculated using the rate constant of reaction (2).[12]

N_2^1 First Negative Band System Radiation

The approximative scheme of an electronic–vibrational excited state of the nitrogen molecular ion $N_2^+(B^2\Sigma_u^+)$ formation was used to calculate the radiation in the first negative band system N_2^+. The second electronic excited state of N_2^+ can be populated in the reactions (Table 8).

In Table 8, $N_2^+(X) \equiv N_2^+(X^2\Sigma_g^+)$, $N_2^+(A) \equiv N_2^+(A^2\Pi_u)$, $N_2^+(B) \equiv N_2^+(B^2\Sigma_u^+)$. The radiative decay of $N_2^+(A)$ excited ions is neglected.

Results

In Fig. 4, the calculated radiation intensity of NO(γ) (λ = 235 ± 7 nm, P_1 = 0.1 torr, V_s = 8 km/s) behind a strong shock

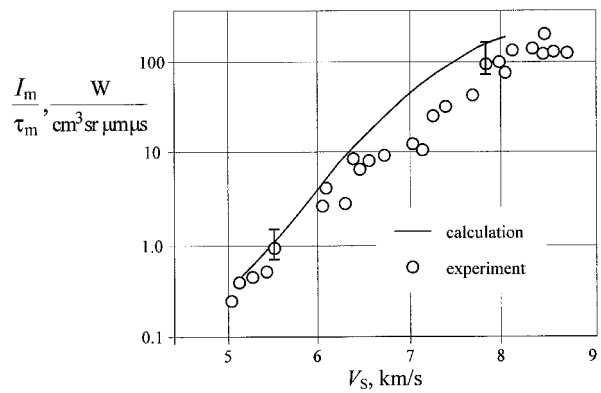

Fig. 6 NO(g) radiation intensity peak rise as a function of shock-wave velocity: l = 235 ± 7 nm, P_1 = 0.1 torr.

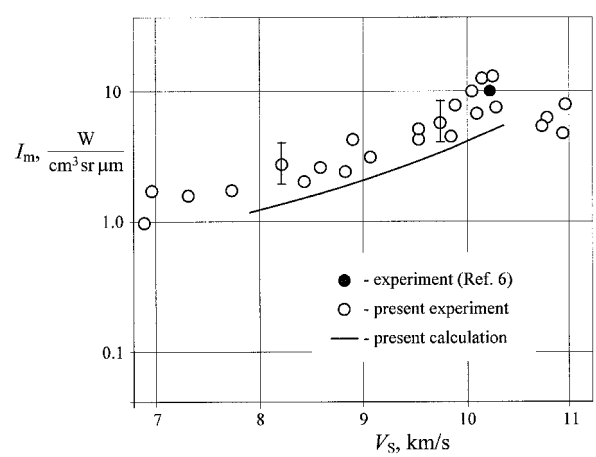

Fig. 7 $N_2^+(12)$ radiation intensity peak as function of shock-wave velocity: l = 391.4 ± 0.2 nm, P_1 = 0.1 torr.

wave is compared with the experimental data corrected by the instrument function. One can see that calculated and experimental maximum emission intensity I_m and the decrease rate of the nonequilibrium peak of radiation intensity satisfactorily agree. The measured time of the I_m achievement is more than the calculated one. Note that a numerical model shock wave radiation (SWR) doesn't take the front structure of a shock wave into account, and the finite time of the translational temperature rise, which can be about 0.3 μs (Ref. 15) (laboratory coordinate system) under experimental conditions. (In Ref. 5, the comparison of measured and calculated profiles of radiation intensity was made with the assumption that measured and calculated times of the I_m achievement are equal.) Dependence of the maximum radiation level at the nonequilibrium peak (λ = 235 ± 7 nm), on the shock wave velocity $I_m = f(V_s)$ is presented in Fig. 5, where the experimental results and corresponding calculations (taking into account an instrument function of the measurement system) are shown. Calculated data agree with measurements. The increase of radiation behind the shock wave can be characterized by the value of I_m/τ_m, where τ_m is the time of the radiation maximum achievement behind a shock-wave front. The function $I_m/\tau_m = f(V_s)$, ob-

tained from the experimental results and calculations for λ = 235 ± 7 nm and P_1 = 0.1 torr, is shown in Fig. 6. The measured function $I_m = f(V_s)$ at the nonequilibrium peak in the spectral interval λ = 391.4 ± 0.2 nm [$N_2^+(1-)$ system] is shown in Fig. 7. Comparison of the radiation peak intensity measurements at $\lambda \sim 391.4$ nm, the experimental data presented in Ref. 6 for V_s = 10.2 km/s, and our calculation data using the SWR model show good agreement with measured data. The measured data I_m lie slightly above the calculated value. Note the decrease in I_m at $V_s > 10$ km/s. However, the detailed investigation of radiation particularities at $V_s > 10$ km/s is not discussed in this paper.

Viscous Shock-Layer Radiation

Calculation studies of hypersonic viscous shock-layer radiation have been performed on the numerical solution of Navier–Stokes equations. In these studies a simplified kinetic model was adequate during the calculations of nonequilibrium processes behind the strong shock wave. A multicomponent mixture described in the preceding text was considered. The nonequilibrium excitation of vibrational levels was taken into account by the introduction of vibrational temperatures for T_{vN_2}, T_{vO_2}, and T_{vNO}. The molecule vibration–dissociation coupling model from Ref. 7 was used in the numerical model. Only associative ionization processes were considered. The electron temperature and the nitrogen vibrational temperature were assumed to be equal. Transport coefficients have been calculated from the Wilke and Masone–Saxena formula. In doing so, the Lennard-Jones potential was used. When solving a hypersonic streamlining problem, Rankine–Hugoniot generalized conditions were used on a shock wave, and the conditions of no-slip local heat balance, catalycity, and the equilibrium condition $T_v = T$ were used on a wall. A fully implicit integro-interpolation method was used. To solve nonlinear grid equations, a Newton–Rafson modified method was used, and the solution of a linearized system of grid equations was made by lower-upper (LU) decomposition, with a preliminary numbering of the unknowns by the area-rule concept. A more complete description of the computational method for viscous layer calculations is presented in Ref. 13. Calculation results on the distribution of translational and vibrational temperatures T, T_{vO_2}, T_{vN_2}, and T_{vNO}, and the charge species densities in the shock layer for the flight at H = 80 km, at V = 8.0 km/s, and a fully catalytic streamlined surface are shown in Fig. 8. Shock-layer emission spectra of the NO band systems for the stagnation streamline calculated for these conditions are shown in Fig. 9. Calculations of the viscous shock-layer radiance for Bow Shock-1 (V = 3.5 km/s) and Bow Shock-2 (V = 5.1 km/s) vehicles are shown in Fig. 10. Shock-layer radiance calculation for λ = 230 ± 25 nm is compared with the Navier–

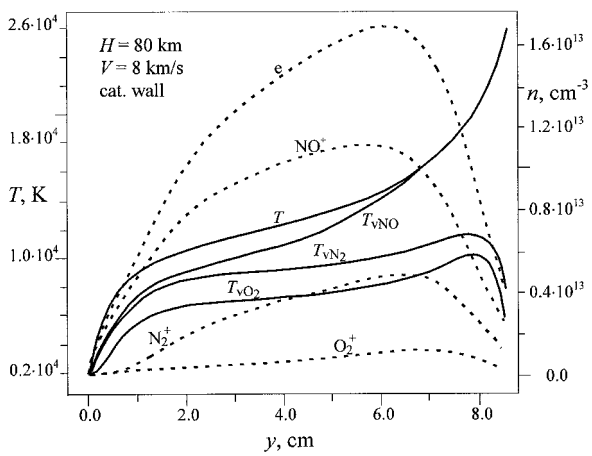

Fig. 8 Stagnation streamline temperatures and charge species concentrations profiles (V 5 8 km/s, H 5 80 km).

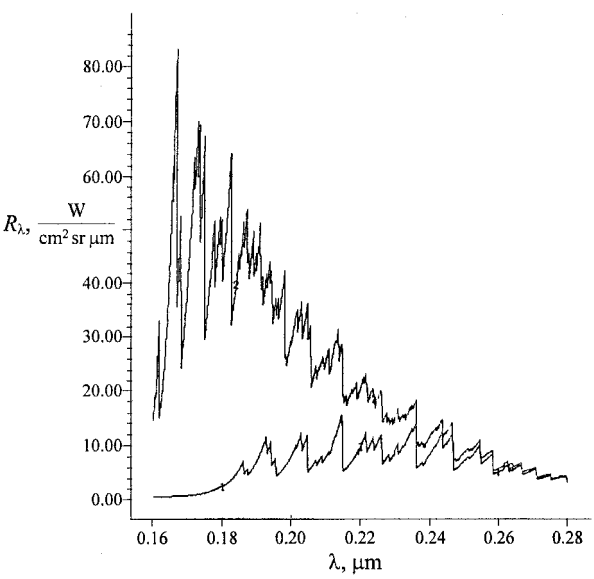

Fig. 9 NO uv emission spectra in viscous shock layer (V 5 8 km/s, H 5 80 km), 1 2 NO(g) radiance, 2 2 NO(b) + NO(g) 1 NO(d) 1 NO(α) radiance.

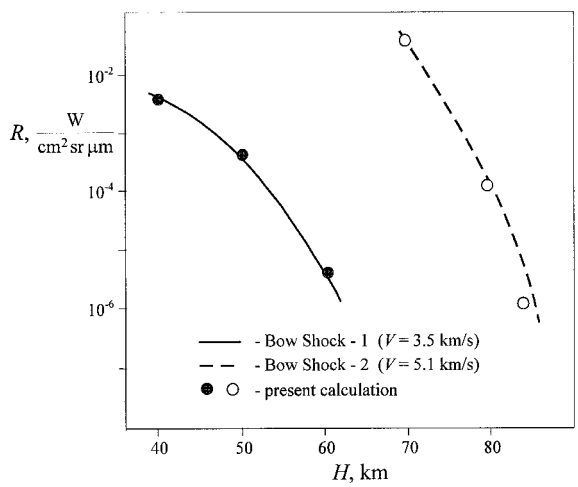

Fig. 10 Comparison of radiance obtained by the present calculations and flight measurements from Ref. 2.

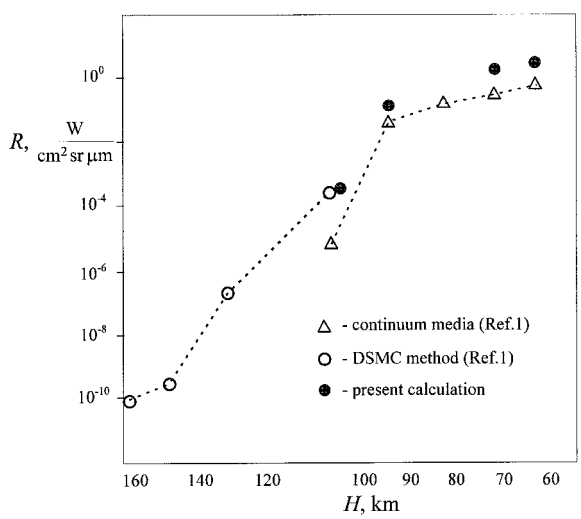

Fig. 11 Comparison of radiance obtained by the present calculations and calculated data from Ref. 1 for flight conditions (V 5 8.0 km/s and H 5 60–100 km).

Stokes and direct simulation Monte Carlo (DSMC) method numerical data[1] for $H = 100-60$ km at $V = 8$ km/s in Fig. 11. Our calculations suggest an instrument function $f = 1$ when $\lambda = 230 \pm 25$ nm and $f = 0$ outside this interval.

Conclusions

The complex method when the numerical simulation of the nonequilibrium radiative processes was accompanied by experimental investigations in EAST, was elaborated to determine the NO and $N_2^+(1-)$ nonequilibrium emission in the shock layer in air. The kinetics is based on the main part of the data bank, where the results by Russian scientists are generally used. Attention was paid to the multitemperature kinetical schemes when the difference between translational, vibrational, and electron temperatures, and level's model of the electronic–vibrational excited states of the NO and $N_2^+(1-)$ formation with the resonant energy exchange reactions were taken into account. The comparative analysis showed the successful agreement between measured and calculated data on the radiation intensity for the $N_2^+(1-)$ band system. Models of an NO uv-emission formation is in a good agreement with the flight experiments for flight velocities $V = 3.5$ and 5.1 km/s and laboratory measurements in EAST at $V_s = 5$ and 8 km/s, but the model needs some corrections in the shock-wave 6–7 km/s velocities range. The NO uv emission is sensitive to the resonant energy exchange reactions with nitric oxide and metastable N_2 molecules participation and to the variation of the rate constants for fast reactions of NO formation. It is necessary to consider the particularities of the kinetical processes in the thermononequilibrium zone of the shock-wave front to determine the radiation peak in this zone. Additional measurements are required to study the peculiarities of the radiation formation processes in the shock-front region.

Acknowledgments

This work was supported by the U.S. Army Research Office and managed by the U.S. Air Force Arnold Engineering and Development Center. The experimental part of this investigation was supported by Grant 96-01-00565 of the Russian Fund of Fundamental Investigations. The authors thank Lilia A. Kildushova, Olga L. Chernova, Sergej V. Chernov, and Vadim G. Tchebureev for their assistance.

References

[1]Levin, D. A., Finke, R. G., Candler, G. V., Boyd, I. D., Howlet, C. L., Erdman, P. W., and Zipf, E. C., "In-Situ Measurements of Transitional and Continuum Flow UV Radiation from Small Satellite Platforms," AIAA Paper 94-0248, Jan. 1994.

[2]Levin, D. A., Candler, G. V., Collins, R. J., Erdman, P. W., Zipf, E. C., and Howlet, C. L., "Examination of Ultraviolet Radiation Theory for Bow Shock Rocket Experiments," AIAA Paper 92-2871, July 1992.

[3]Anon., "Russian Aeronautical Test Facilities," ANSER Center for International Aerospace Cooperation, Arlington, VA, 1995.

[4]Gorelov, V. A., Kildushova, L. A., and Kireev, A. Y., "Ionization Particularities Behind Intensive Shock Waves in Air at Velocities of 8–15 km/s," AIAA Paper 94-2051, June 1994.

[5]Gorelov, V. A., Gladyshev, M. K., Kireev, A. Y., Yegorov, I. V., Plastinin, Y. A., and Karabadzhak, G. F., "Nonequilibrium Shock-Layer Radiation in the Systems of Molecular Bands NO and $N_2^+(1-)$: Experimental Study and Numerical Simulation," AIAA Paper 96-1900, June 1996.

[6]Sharma, S. P., and Whiting, E. E., "Modeling of Nonequilibrium Radiation Phenomena. An Assessment," AIAA Paper 94-0253, Jan. 1994.

[7]Losev, S. A., Makarov, V. N., Pogosbekyan, M. J., Shatalov, O. P., and Nikol'sky, V. S., "Thermochemical Nonequilibrium Kinetic Models in Strong Shock Waves in Air," AIAA Paper 94-1990, June 1994.

[8]Park, C., "Review of Chemical-Kinetic Problems of Future NASA Missions, I: Earth Entries," *Journal of Thermophysics and Heat Transfer*, Vol. 7, No. 3, 1993, pp. 385–398.

[9]Schultz, G. J., "Vibrational Excitation of N_2, CO and H_2 by Electron Impact," *Physical Review*, Vol. 135, No. 4A, 1966, pp. 531–536.

[10]Mihailov, A. A., and Pivovar, V. A., "Model Calculation of Rate Constants Step-by-Step Excitation of Vibrational Levels of Nitrogen by Electron Impact," *Soviet Journal of Technical Physics*, Vol. XLV, No. 5, 1975, pp. 1063–1068 (in Russian).

[11]Treanor, C. E., Adamovich, I. V., Williams, M. J., and Rich, J. W., "Kinetics of NO Formation Behind Strong Shock Wave," AIAA Paper 95-2061, June 1995.

[12]Bose, D., and Candler, G. V., "Thermal Rate Constants of the $N_2 + O \rightarrow NO + N$ Reaction Using *ab initio* $^3A''$ and $^3A'$ Potential Energy Surfaces," *Journal of Chemical Physics*, Vol. 104, No. 8, 1996, pp. 2825–2833.

[13]Kasyanov, V. A., and Podlubny, L. I., "About the Theory of Associative Ionization," *Moscow Energetic Institute Scientific Conference Proceedings, Series Physical*, MEI Publ., Moscow, 1967, pp. 131–141 (in Russian).

[14]Smirnov, B. M., *Atomic Collisions and Elementary Processes in Plasma*, Atomizdat, Moscow, 1968 (in Russian).

[15]Carlson, A. B., and Hassan, H. A., "Direct Simulation of Re-Entry Flow with Ionization," *Journal of Thermophysics and Heat Transfer*, Vol. 6, No. 3, 1992, pp. 400–404.

[16]Kamenschikov, V. A., Nikolaev, V. M., and Plastinin, Y. A., *Radiative Properties of Gases at High Temperatures*, Mashinostroenie, Moscow, 1971 (in Russian).

[17]Kuznetsova, L. A., Kuzmenko, N. E., Kuziakov, Y. Y., and Plastinin, Y. A., *Probabilities of Optical Transitions of Diatomic Molecules*, Nauka, Moscow, 1980 (in Russian).

[18]Kuznetsova, L. A., Kuzmenko, N. E., and Kuziakov, Y. Y., *Frank-Condon Factors for Diatomic Molecules*, Moscow State Univ., Moscow, 1984 (in Russian).

[19]Yegorov, I. V., "The Numerical Simulation of Vibration-Dissociation Interaction at Hypersonic Overflow," AIAA Paper 96-1894, June 1996.

[20]Gross, R. W. F., and Cohen, N., "Temperature Dependence of Chemiluminescent Reactions II. Nitric Oxide Afterglow," *Journal of Chemical Physics*, Vol. 48, No. 6, 1968, pp. 2582–2590.

[21]Pravilov, A. M., *Photo-Processes in Molecular Gases*, Energoatomizdat, Moscow, 1992 (in Russian).

[22]Povch, M. M., and Skubenich, V. V., "NO Electronic States Excitation by Electron Impact," *Proceedings of the 8th International Conference on Phenomena in Electron—Atomic Collisions*, Vol. 1, GK Publishing House, Beograd, Yugoslavia, 1973, pp. 383, 384.

[23]Smirnov, Y. M., "Experimental Study of Molecular Electronic States Step-by-Step Excitation by Electron Impact (Atmospheric Gases)," *Proceedings of the 11th Soviet Conference on Electron-Atomic Collisions*, Uzhgorod, USSR, June 1988, pp. 67–69 (in Russian).

[24]Smirnov, B. M., *Ions and Excited Atoms in Plasma*, Atomizdat, Moscow, 1974 (in Russian).

[25]Drakes, J. A., McGregor, W. K., and Mason, A. A., "Two-Electron Exchange in Collisions of Neutral Molecules," *Journal of Chemical Physics*, Vol. 99, No. 10, 1993, pp. 7813–7818.

[26]Kurochkin, Y. M., Polak, L. C., Pustogarov, A. B., Slovetsky, D. I., and Ukolov, V. V., "Mechanism of Particles Excitation in Nitrogen Plasma," *High Temperature*, Vol. 16, No. 6, 1978, pp. 1167–1177 (in Russian).

[27]Smith, G. P., Crosley, D. R., and Eckstrom, D. J., "Mechanism and Rate Constants for the Chemistry of Radiating, Shock-Heated Air," SRI Project, 6277, MP 89-037, Feb. 1989.

[28]Berdichevsky, M. G., and Marusin, V. V., "The Influence of the Metastability of $A\,^3\Sigma_u^+$ Nitrogen State on Step-by-Step Excitation Processes in Nitrogen Plasma," *Soviet Journal of Applied Spectroscopy*, Vol. 20, No. 2, 1974, pp. 187–195 (in Russian).

[29]Polak, L. C., Slovetsky, D. I., Urbas, A. D., and Fedoseeva, T. V., "Relaxation Measurements and Mechanisms of Excitation of Electron-Vibrational States of Molecules in Nitrogen Plasma," *Plasma Chemistry*, Vol. 5, edited by B. M. Smirnov, Atomizdat, Moscow, 1978, pp. 242–280 (in Russian).

[30]Cartwright, D. C., "Rate Coefficients and Inelastic Momentum Transfer Cross Sections for Electronic Excitation of N_2 by Electrons," *Journal of Applied Physics*, Vol. 49, No. 7, 1978, pp. 3855–3862.

[31]Ivanov, E. E., and Chernyshova, N. V., "Step-by-Step Excitation of $N_2(B)$ in Decay Plasma," *Proceedings of the 15th International Conference on Phenomena in Ionized Gases*, Pt. 1, VINITI Publishing, Minsk, 1981, pp. 409–410.

[32]McConkey, J. W., Woolsey, J. M., and Burns, D. J., "Absolute Cross Section for Electron Impact Excitation of 3914 Å N_2^+," *Planetary and Space Science*, Vol. 19, No. 9, 1971, pp. 1192–1198.